Supporting Information

The thermophilic biomass-degrading bacterium *Caldicellulosiruptor bescii* utilizes two enzymes to oxidize glyceraldehyde-3-phosphate during glycolysis

Israel M. Scott[1§], Gabriel M. Rubinstein[1§], Farris L. Poole II[1], Gina L. Lipscomb[1], Gerrit J. Schut[1], Amanda M. Williams-Rhaesa[2], David M. Stevenson[3] , Daniel Amador-Noguez[3], Robert M. Kelly[4] and Michael W. W. Adams[1]*

[1]Dept. of Biochemistry and Molecular Biology, University of Georgia,

Athens, GA 30602, USA

[2]New Materials Institute, University of Georgia, Athens, GA 30602, USA

[3]Dept. of Bacteriology, University of Wisconsin-Madison, Madison, WI 53706, USA

[4]Dept. of Chemical and Biomolecular Engineering, North Carolina State University, Raleigh, NC 27695,

USA

[§]These authors contributed equally to this work

*To whom correspondence should be addressed:

Michael W. W. Adams (adamsm@uga.edu)

Supplementary Tables S1-S5 and Figures S1-S10

Table S1. Protein concentration dependent activity of GOR

Enzyme Assay	[GAP] (mM)	GOR (mg)	Total Activity (U)	Specific Activity (U/mg)
GOR	1	0	0	0.0
GOR	1	0.005	0.31	61.3
GOR	1	0.010	0.62	61.7
GOR	1	0.015	0.92	61.6

Standard assays were conducted with 1 mM BV in 2 mL of 50 mM EPPS buffer, pH 8.0, in sealed anaerobic cuvettes. Reactions were carried out with varying concentrations of purified His-tagged GOR and reactions were initiated by the addition of GAP. Increasing concentrations of enzyme increased the total BV reduction activity, but specific activity remained constant. Without the addition of GOR, no GAP dependent reduction of BV was observed, demonstrating that GOR is responsible for the measured activity.

Table S2. Effect of TPI on standard GAPDH and GOR activities

Enzyme Assay	TPI	[GAP] (mM)	[DHAP] (mM)	Predicted Activity	Specific Activity (U/mg)
GOR	-	0	10	No	0.0
GOR	-	1	0	Yes	61.3
GOR	-	1	1	Yes	47.6
GOR	-	1	10	Yes	18.1
GOR	+	0	10	Yes	16.7
GOR	+	1	0	No	1.5
GOR	+	5	0	Yes	190.1
GOR	+	15	0	Yes	645.5
GAPDH	-	1	0	Yes	0.9
GAPDH	-	0	10	No	0.1
GAPDH	-	1	10	Yes	4.4
GAPDH	+	0	10	Yes	2.6
GAPDH	+	1	0	No	0.0
GAPDH	+	5	0	Yes	2.2
GAPDH	+	15	0	Yes	23

Standard GOR and GAPDH assays were performed in sealed anaerobic cuvettes in 2 mL of EPPS buffer, pH 8.0. GOR assay included 1 mM BV and 0.005 mg of purified His-tagged GOR. GAPDH assays included 20 mM dipotassium phosphate, 1 mM NAD and 20 μL of partially purified GAPDH (1.6 mg/mL). Reactions marked "+" contained 30 uL of partially purified TPI (10 mg/mL) while those designated "-" did not include TPI (although minor TPI contamination of GAPDH is indicated by background activity when DHAP but no GAP was added). Reactions containing GAP were initiated by the addition of GAP to the assay mixture. Reactions containing containing TPI but no GAP were initiated by the addition of TPI. Specific activity is expressed per mg of GOR or GAPDH.

Table S3. Strains used and constructed in this study

Strain	Parent	Genotype	Alias	Reference
MACB1032		*ΔpyrE ΔcbeI*		(1)
JWCB018		*ΔpyrFA ΔcbeI*		(2)
MACB1010	JWCB018	*ΔpyrFA ΔcbeI:*P_{slpr}*xor-pfd*	OE-XOR/PFD	This study
MACB1050	MACB1032	*ΔpyrE ΔcbeIΔgorL*	*ΔgorL*	This study
MACB1074	MACB1032	*ΔpyrE ΔcbeIΔgorS*	*ΔgorS*	This study

Table S4. MS-based metabolomics of Δ*gorL* and parent strains

Metabolite	Log_2 Fold change[a]
Homocysteine	3.555 ± 0.363
Ribose 5-phosphate	1.675 ± 0.234
Sedheptulose 7-phosphate	1.614 ± 0.179
4-hydroxybenzoate	1.478 ± 0.276
Glucose-6-phosphate	1.341 ± 0.097
Fructose 6-phosphate	1.318 ± 0.082
Malate	0.916 ± 0.026
Ribulose 5-phosphate	0.892 ± 0.267
Glycerol-3-phosphate	0.525 ± 0.016
Fructose 1_6-bisphosphate	0.505 ± 0.06
Dihydroxy acetone phosphate	0.485 ± 0.013
Threonine	0.477 ± 0.069
Valine	0.278 ± 0.04
Phenylalanine	0.253 ± 0.015
Myoinositol	0.238 ± 0.005
Glutamate	0.164 ± 0.006
Serine	0.164 ± 0.044
Leucine	0.044 ± 0.001
Succinate	0.002 ± 0
Pyruvate	-0.019 ± 0.001
UDP-N-acetylglucosamine	-0.127 ± 0.005
Phenylpyruvate	-0.177 ± 0.005
Methionine	-0.354 ± 0.029
Aspartic acid	-0.445 ± 0.022
2-ketoglutarate	-0.454 ± 0.031
Tyrosine	-0.772 ± 0.030
Dihydroorotate	-0.820 ± 0.046
Isoleucine	-1.071 ± 0.012
Fumarate	-1.326 ± 0.135
NAD+	-1.407 ± 0.145
Citrate	-1.769 ± 0.022
Quinolinate	-2.060 ± 0.824
3-phosphoglycerate	-4.122 ± 0.142
Phosphoenolpyruvate	-4.525 ± 0.178

[a]Changes in concentration are given relative to the parent strain.

Table S5. Primers used in this study

Primer	Target locus	Sequence (5'-3')
ISAORKO3'F	3' flank *gor*-L	AAGTTAGGCTGGTGGGTACCTTCCCAAATCTGCACCCTATC
JAB0004	3' flank *gor*-L	CAAAAAAACTATTTACCTCTACTCCAATCTTCATTTAAAATGGAATTCTTTTTGAAAC
JAB0003	pAR003	TTAAAATGGAATTCTTTTTGAAACATCAAC
JAB002	pAR003	CTGCATAGCCTCTTTTAAATCCTGTCTTACTCACTCACCTCTTCCATTG
JAB001	5' flank *gor*-L	CTTACTCACTCACCTCTTCCATTG
ISAORKO5'R	5' flank *gor*-L	GGACTATGAAGGAGAGCTGAATTCTCTGACGCTCAGT
ISAORKOvectorF	pGL104(1)	TGAATTCTCTGACGCTCAG
ISCB003	pGL104	CTTTCTACATAGAAAGGATGGTCTCTAGAATGAATAAAGATGCTTACATTCAAATGTTC
GLCB096	pGL104	ATGAATAAAGATGCTTACATTCAAATGTTC
ISAORKOvectorR	pGL104	GTTAGGCTGGTGGGTACC
ISCB004	pims006	CATAGCCTCTTTTAAATCCTGT
JAB0003	pims006	TTAAAATGGAATTCTTTTTGAAACATCAAC
ISCB005	5' flank *gor*-S	CATAGCCTCTTTTAAATCCTGTTTAAATCACCACCTGTAAAATC
ISCB006	5' flank *got*-S	GGAAAGCTTATTAATTATGTAAAATAAGAATTCTCTGACGCTCAG
ISCB007	pims006	GAATTCTCTGACGCTCAG
ISCB008	pims006	GTTAGGCTGGTGGGTACC
ISCB009	3' flank *gor*-S	CTTATAAAGTCTTTGCCTATCATTTAAAATGGAATTCTTTTTGAAAC
ISCB010	3' flank *gor*-S	GTTAGGCTGGTGGGTACCCTGTTGTCTTTATCCCCAAAAG
IS AORKOvectorR2	pIMSPFAOR	CCAATGATCGAAGTTAGGCTGGTGGTACCTTATTTTACATAATTAATAAG
IS AORKOvectorF2	pIMSPFAOR	GCAGATAGAAGGAATTCTCTGACGCTCAGTGGAAC
IS tagAOR5'F2	5' flank *gor*-S	CGAAGTTAGGCTGGTGGTACCTTATTTTACATAATTAATAAGCTTTCC
IS tagAOR5'R	5' flank *gor*-S	GGTTCTTCGAGCTGATAACACAGGATTTA

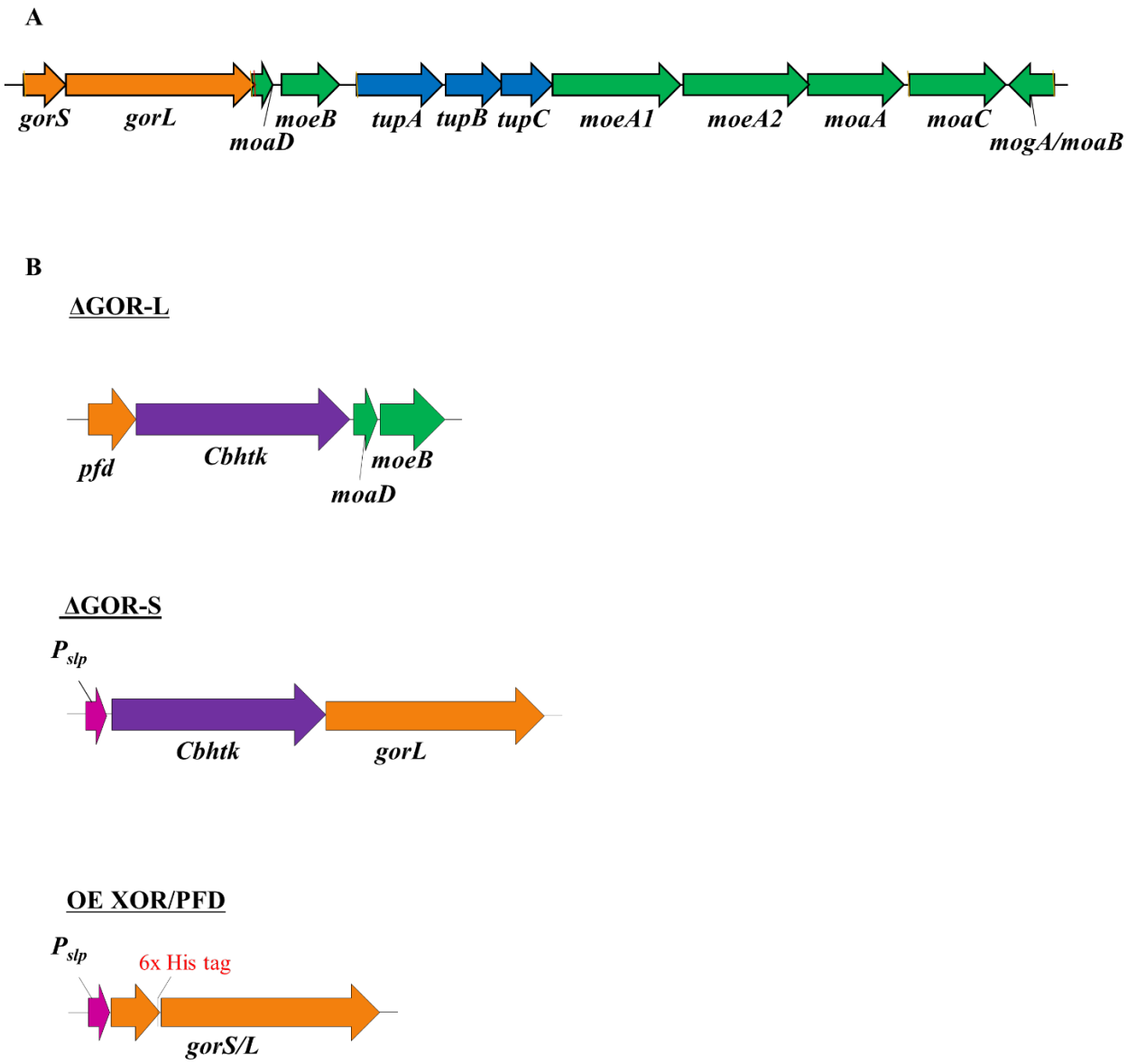

Figure S1. A) *C. bescii* gene cluster (Athe_0820 to Athe_0831) encoding GOR-L and GOR-S (orange) and the proteins necessary for pyranopterin biosynthesis (green) and tungstate transport (blue). B) Gene organization of recombinant strains of *C. bescii* Δ*gorL* (MACB1050), Δ*gorS* (MACB1074) and OE-XOR/PFD (MACB1010). Abbreviations: slp, S-layer protein; Cb*htk*, thermostable kanamycin resistance gene.

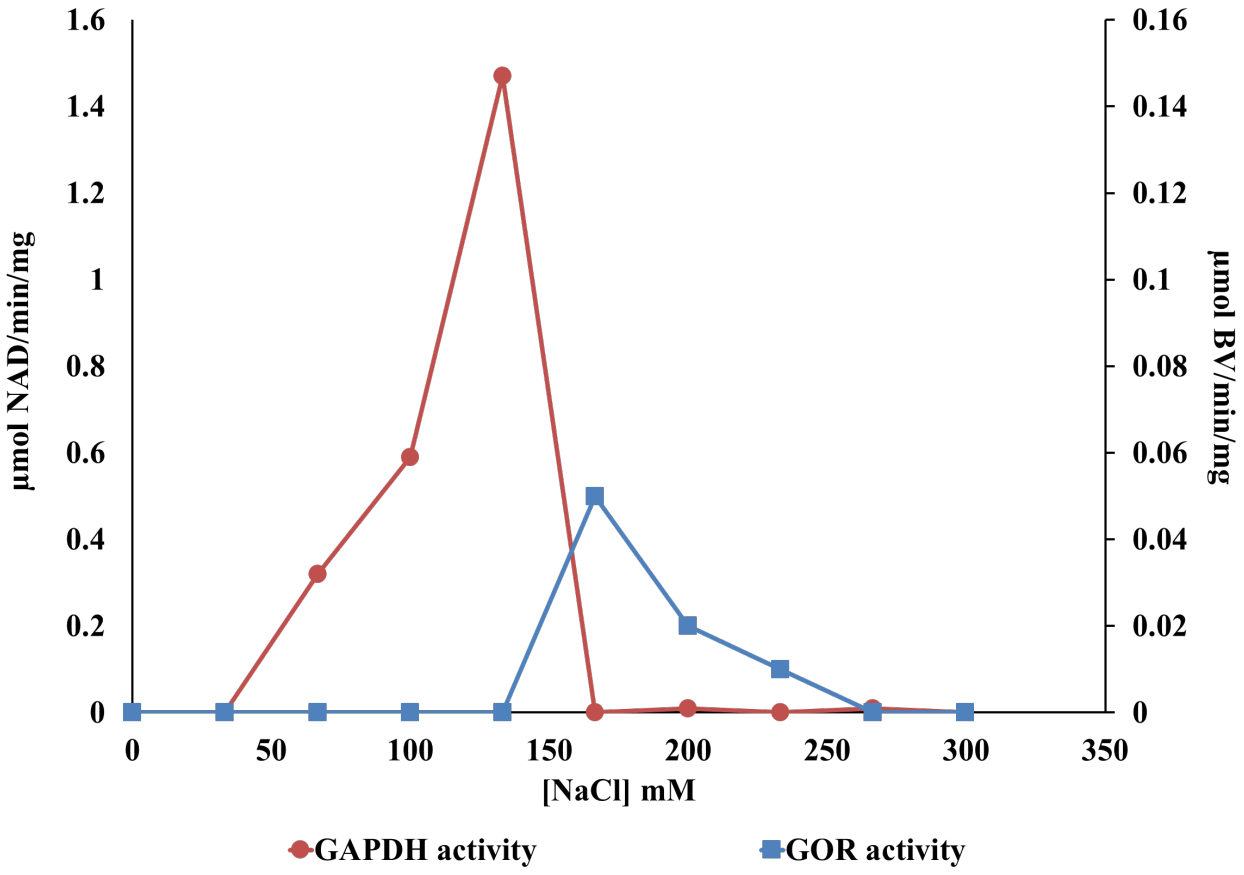

Figure S2. Activity of GOR and GAPDH following separation by anion exchange chromatography. The activity of GAPDH (red) and GOR (blue) were determined by the GAP-dependent reduction of NAD and benzyl viologen (BV), respectively. The concentrations were GAP (5 mM), NAD (1 mM) and BV (1 mM).

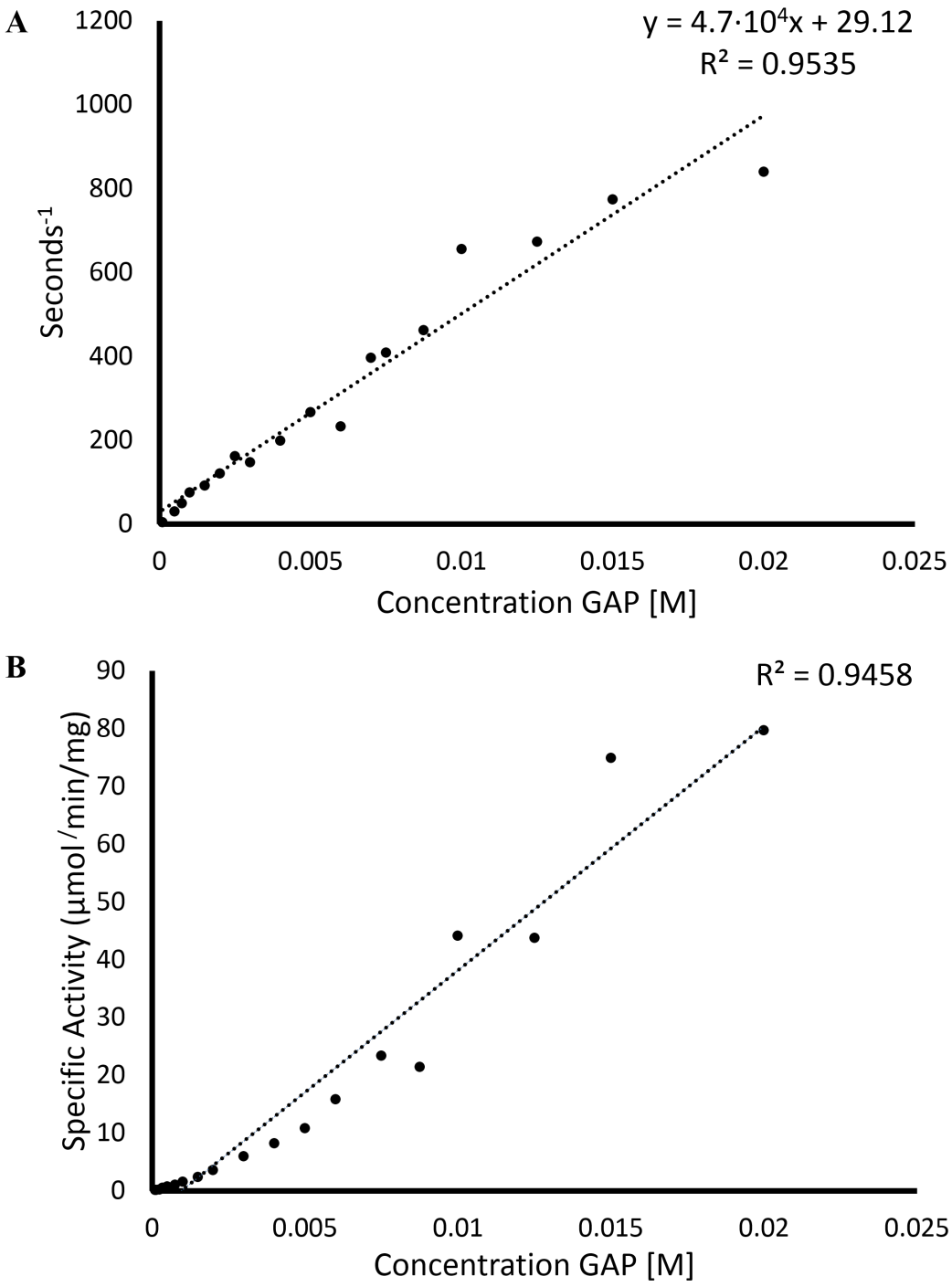

Figure S3. Kinetic properties of purified GOR (A) and partially purified GAPDH (B). The activities were measured by reduction of BV and NAD, respectively, both at a concentration 1 mM.

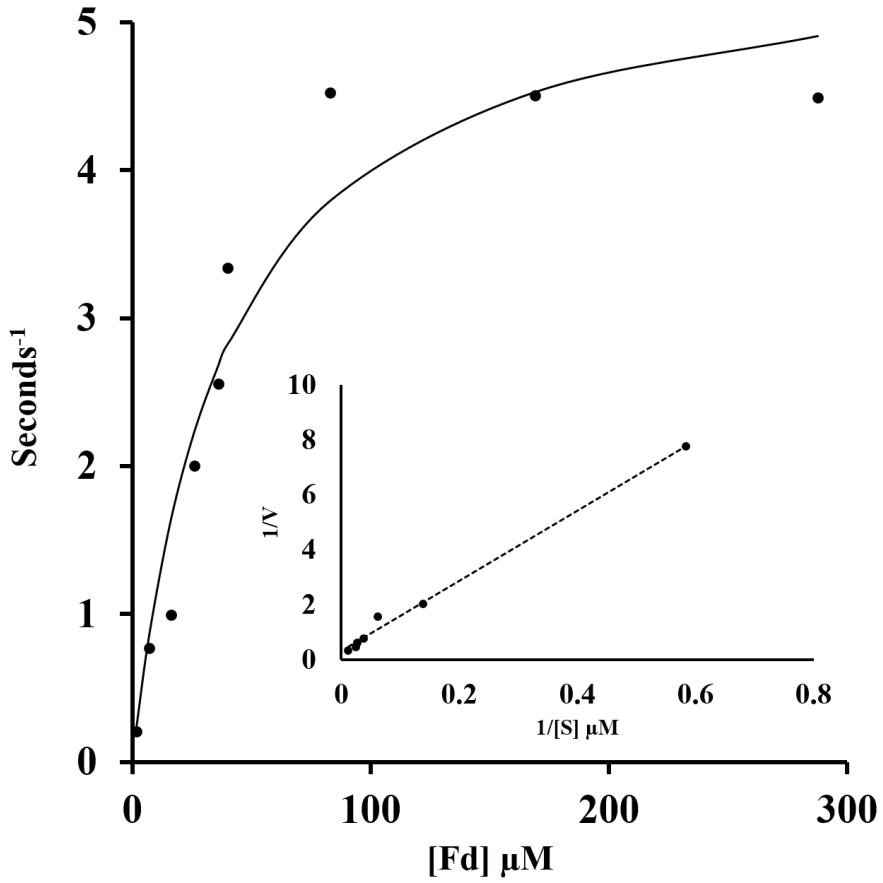

Figure S4. Kinetic properties of purified GOR using *C. bescii* ferredoxin as the electron acceptor. The concentration of GAP was 5 mM.

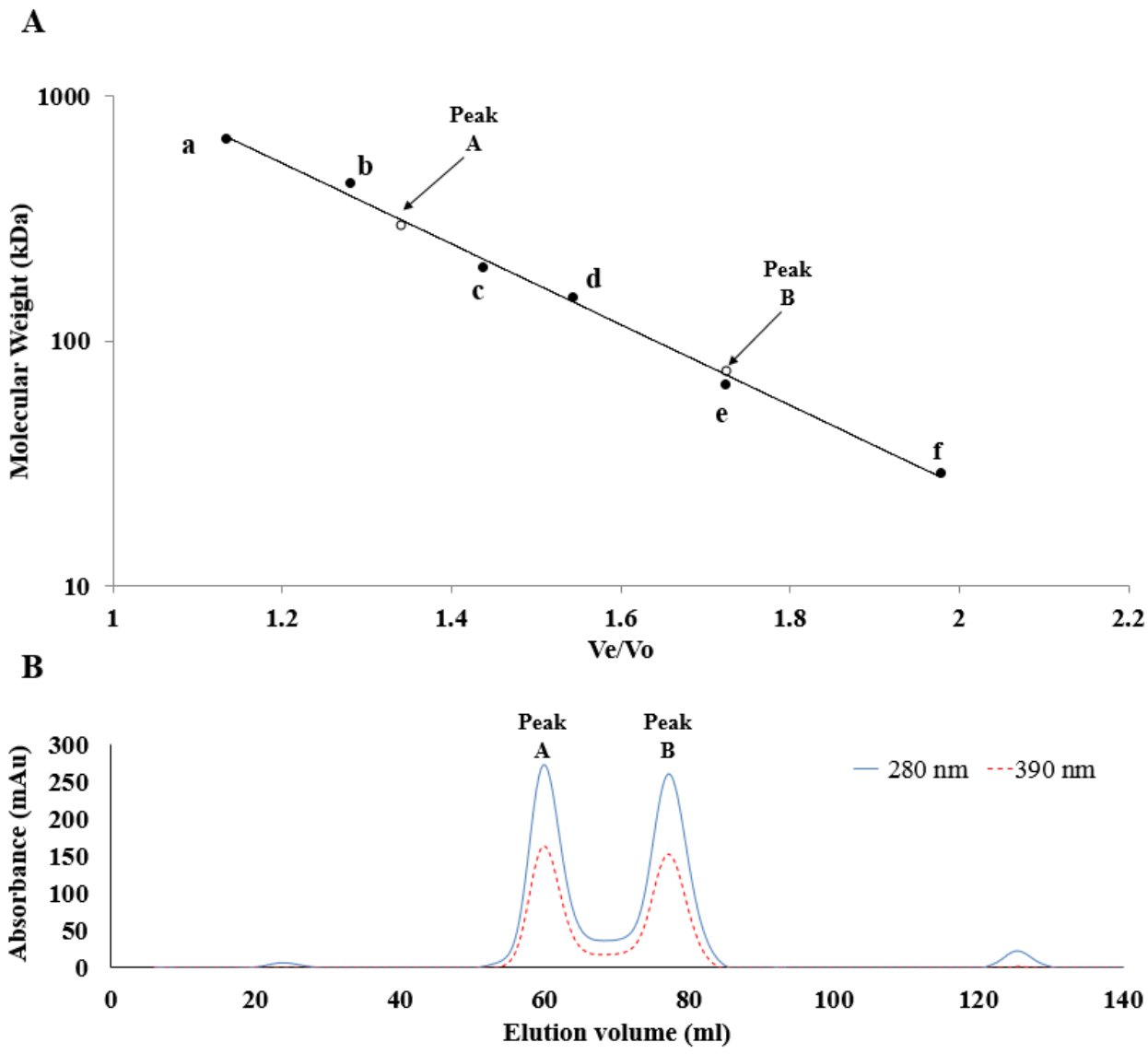

Figure S5. A) Estimated molecular mass of GOR holoenzyme (Peak B) and GOR heterodimer (Peak A; open circles/arrows). The standard proteins (closed circles) are (a) thyroglobulin (669 kDa), (b) apoferritin (443 kDa), (c) amylase (200 kDa), (d) alcohol dehydrogenase (150 kDa), (e) albumin (66 kDa) and (f) carbonic anhydrase (29 kDa). B) Size exclusion chromatography elution profile of affinity purified GOR showing GOR holoenzyme (Peak B) and GOR heterodimer (Peak A). Fractions were monitored in the UV (280 nm for protein) and visible (390 nm for iron-sulfur clusters) regions.

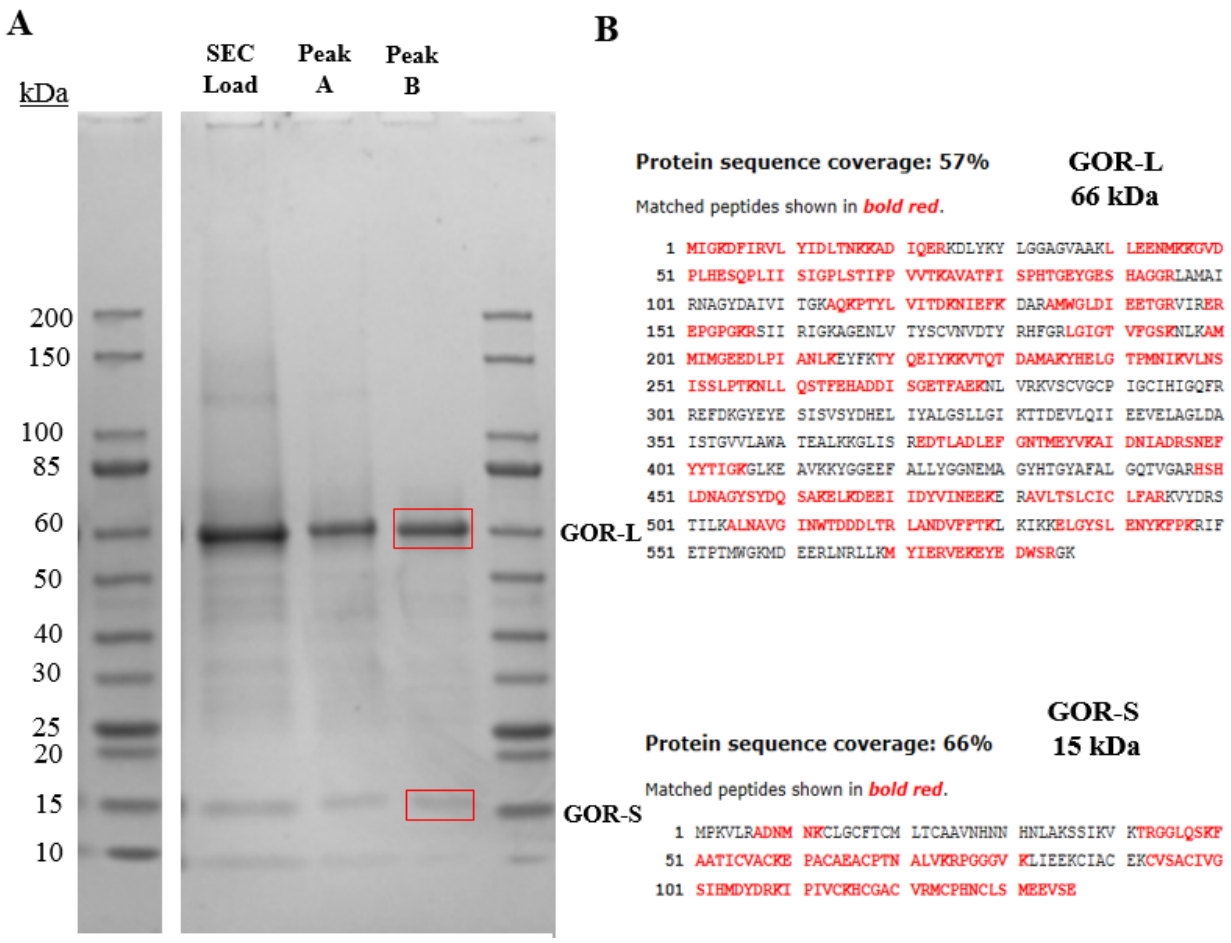

Figure S6. A). SDS-PAGE analysis of GOR following ion exchange, affinity and size exclusion chromatography steps from cell extract of the *C. bescii* strain OE-XOR/PFD. Lane 1 affinity purified GOR lanes 2 and 3, peaks A and B respectively from size exclusion chromatography (refer to Figure S5B). Gel was stained with Imperial Protein Stain B). MS/MS analysis of the indicated bands. Peptides that matched the sequence of GOR-L and GOR-S are shown in red. Red boxes indicate bands excised for MS analysis.

A

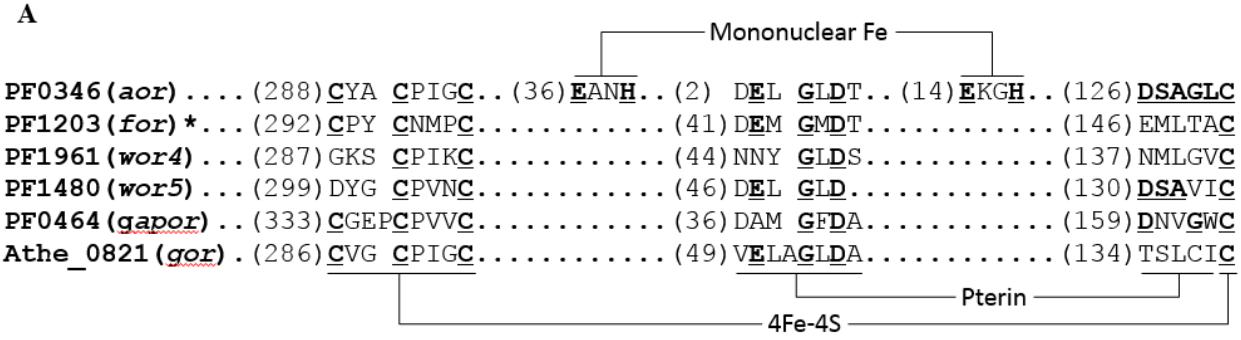

B

MPKVLRADNMNKCLGCFTCMLTCAAVNHNNHNLAKSSIKVKTRGGLQSKFAATICVACKEPACAEACP
TNALVKRPGGGVKLIEEKCIACEKCVSACIVGSIHMDYDRKIPIVCKHCGACVRMCPHNCLSMEEVSE

Figure S7. A). Pterin and [4Fe-4S]-binding motifs in the WOR family enzymes. B). Sequence of GOR-S showing the four cysteine motifs.

*The NCBI RefSeq protein start position shown here for FOR (PF1203) differs from that of the previously purified protein, which contains an additional eight residues at the N-terminus (3).

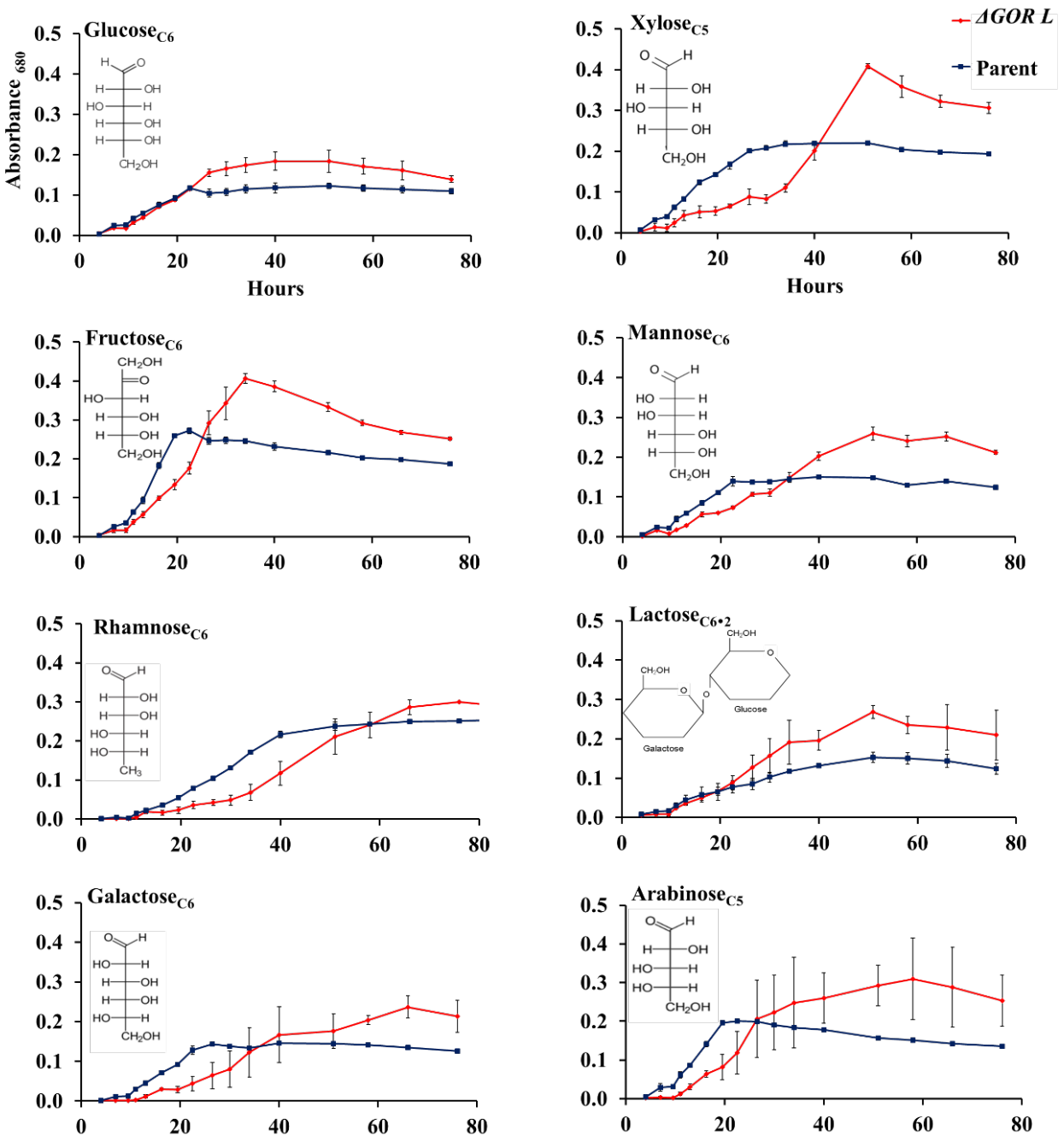

Figure S8. Growth of the parent (blue) and Δ*gorL* (red) strains on the indicated carbon sources at 75°C (n=3).

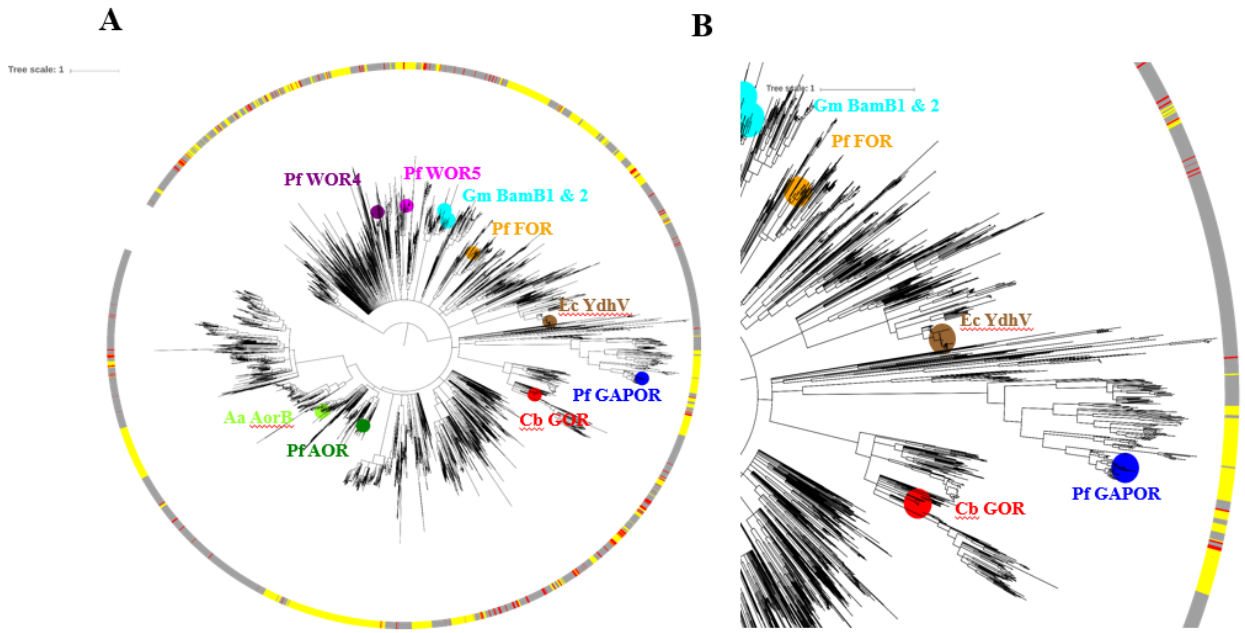

Figure S9. A). Phylogenetic tree of the WOR family of enzymes 4,063 *C. bescii* GOR-L sequence homologs based on InterPro domains (IPR013983 and IPR001203). Only branches with ultrafast bootstrap (UFBoot) values greater or equal to 94% confidence are displayed. represent GOR-L (red) and five previously identified *P. furious* tungsten-containing oxidoreductase enzymes, AOR (dark green), WOR4 (purple), WOR5 (pink), FOR (gold), GAPOR (blue), and three others, Aa AorB (lime green), Ec YdhV (brown) and Gm BamB 1 & 2 (cyan). The outer ring indicates the source of the sequences where bacteria are gray, archaea are yellow and unknown environmental sequences are red. B). An enlarged region of a phylogenetic tree featuring *C. bescii* GOR (Cb GOR) and *P. furious* GAPOR (Pf GAPOR).

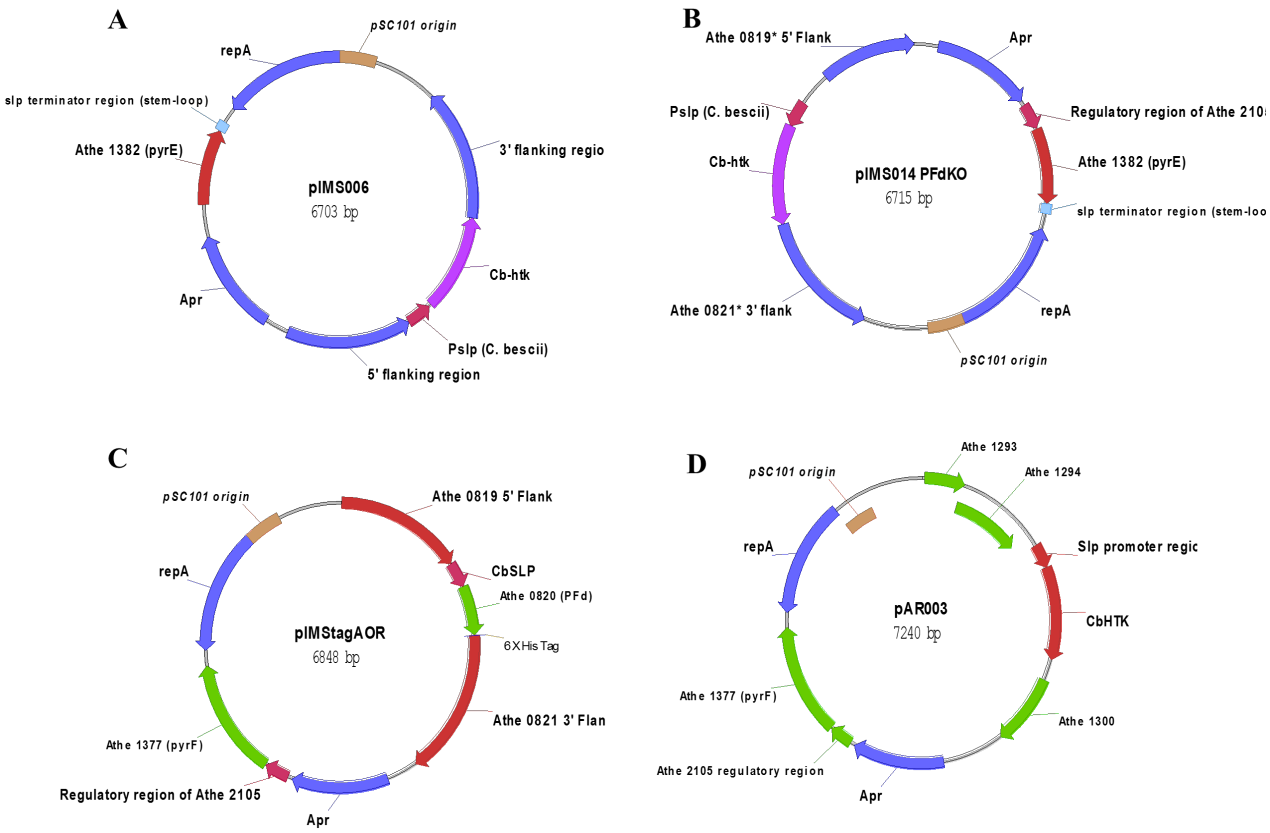

Figure S10. Plasmids used in this study for A) deletion of *gorL* (pIMS006), B) deletion of *gorS* (Pfd; pIMS014) and C) overexpression of His-tagged GOR (pIMStagAOR). CbHTK under control of the slp promoter was cloned from D) (pAP003).

Supplemental References

1. Lipscomb, G. L., Conway, J. M., Blumer-Schuette, S. E., Kelly, R. M., and Adams, M. W. (2016) A highly thermostable kanamycin resistance marker expands the toolkit for genetic manipulation of *Caldicellulosiruptor bescii*. *Appl Environ Microbiol* **82,** 4421-4428
2. Chung, D., Cha, M., Guss, A. M., and Westpheling, J. (2014) Direct conversion of plant biomass to ethanol by engineered *Caldicellulosiruptor bescii*. *Proc Nat Acad Sci* **111**, 8931-8936
3. Roy, R., Mukund, S., Schut, G. J., Dunn, D. M., Weiss, R., and Adams, M. W. (1999) Purification and molecular characterization of the tungsten-containing formaldehyde ferredoxin oxidoreductase from the hyperthermophilic archaeon *Pyrococcus furiosus*: the third of a putative five-member tungstoenzyme family. *J Bacteriol* **181**, 1171-1180